

ORIGINAL ARTICLE

# Efficient gene delivery to the adult and fetal CNS using pseudotyped non-integrating lentiviral vectors

AA Rahim<sup>1,2,3</sup>, AMS Wong<sup>4</sup>, SJ Howe<sup>2</sup>, SMK Buckley<sup>3</sup>, AD Acosta-Saltos<sup>1</sup>, KE Elston<sup>4</sup>, NJ Ward<sup>2</sup>, NJ Philpott<sup>2</sup>, JD Cooper<sup>4</sup>, PN Anderson<sup>5</sup>, SN Waddington<sup>3</sup>, AJ Thrasher<sup>2,6</sup> and G Raivich<sup>1,5</sup>

<sup>1</sup>Perinatal Brain Protection and Repair Group, Department of Obstetrics and Gynaecology, University College London, London, UK;

<sup>2</sup>Molecular Immunology Unit, Centre for Immunodeficiency, Institute of Child Health, University College London, London, UK;

<sup>3</sup>Department of Haematology, Haemophilia Centre and Haemostasis Unit, Royal Free and University College Medical School, London, UK; <sup>4</sup>Pediatric Storage Disorders Laboratory, Department of Neuroscience, Institute of Psychiatry, Kings College London, London, UK;

<sup>5</sup>Department of Anatomy and Developmental Biology, University College London, London, UK and <sup>6</sup>Great Ormond Street Hospital NHS Trust, London, UK

Non-integrating lentiviral vectors show considerable promise for gene therapy applications as they persist as long-term episomes in non-dividing cells and diminish risks of insertional mutagenesis. In this study, non-integrating lentiviral vectors were evaluated for their use in the adult and fetal central nervous system of rodents. Vectors differentially pseudotyped with vesicular stomatitis virus, rabies and baculoviral envelope proteins allowed targeting of varied cell populations. Efficient gene delivery to discrete areas of the brain and spinal cord was observed following stereotactic administration. Furthermore, after direct in utero administra-

tion (E14), sustained and strong expression was observed 4 months into adulthood. Quantification of transduction and viral copy number was comparable when using non-integrating lentivirus and conventional integrating vector. These data support the use of non-integrating lentiviral vectors as an effective alternative to their integrating counterparts in gene therapy applications, and highlight their potential for treatment of inherited and acquired neurological disorders.

Gene Therapy (2009) 16, 509–520; doi:10.1038/gt.2008.186; published online 22 January 2009

**Keywords:** non-integrating lentiviral vectors; central nervous system; fetal gene delivery; pseudotyping

## Introduction

The ability of lentiviral vectors to transduce non-dividing cells, their ease of production and the option to change cell tropism by pseudotyping make them useful gene delivery agents. Recent *in vivo* pre-clinical and clinical trial data have highlighted the potential risk of insertional mutagenesis following integration of retroviral DNA into sensitive areas of the host genome in large animals and humans.<sup>1–3</sup> However, recent studies have also identified this risk using lentiviruses.<sup>4</sup> Non-integrating lentiviruses (NILVs) have been developed by introducing class 1 mutations into the integrase gene, and may obviate some of these difficulties. The vector genome exists episomally as functional double-stranded linear templates or circular forms produced by host nuclear enzymes.<sup>5</sup> In the absence of replication signals, these vectors will eventually be diluted out in dividing cells within a proliferating tissue environment. However, the episomes are retained long term in quiescent or post-mitotic cells.

The central nervous system (CNS) provides an ideal target for NILV vectors because of the post-mitotic status

of mature neurons and relatively slow turnover of glial cells. Recently, Yanez-Munoz *et al.*<sup>6</sup> demonstrated efficient gene delivery and cytomegalovirus (CMV) promoter-driven enhanced green fluorescent protein (EGFP) expression in neuronal cells of the mouse corpus striatum and hippocampus up until the last time point of 30 days using an NI HIV-1-based vector generated with a mutation in the catalytic site of the integrase gene. Philippe *et al.*<sup>7</sup> have also demonstrated expression in striatum using a similar NILV vector but with the <sup>262</sup>RRK integrase mutation. The utility of conventional lentiviral vectors for persistent transduction of the CNS has been explored in several model systems. However, the ability of NILV to reciprocate this activity in various specific anatomical sites and cells specifically with the CNS has not been characterized in detail.

Here we report efficient gene delivery to different cell types within the CNS using variably pseudotyped NILV, as well as long-term gene expression in a mouse *in utero* model. We also show that NILV perform comparably to conventional integrating lentivirus (ILV) in transducing neurons of the CNS.

## Results

### Neural cell-type-specific transduction and gene expression in corpus striatum of adult rats

Variably pseudotyped NILV vectors were injected (2  $\mu$ l) stereotactically into the corpus striatum of adult rats

Correspondence: Dr AJ Thrasher, Molecular Immunology Unit, Centre for Immunodeficiency, Institute of Child Health, 30 Guilford Street, London WC1N 1EH, UK.

E-mail: a.thrasher@ich.ucl.ac.uk

Received 12 June 2008; revised 2 December 2008; accepted 3 December 2008; published online 22 January 2009

( $n = 5$ ). The striatum was chosen as the site of injection due to its relatively large size and ease of access by stereotactic injection. Moreover, this placement allowed detection of any retrograde transport. Thus, retrograde transport of virus from the striatum by nigrostriatal neurons would be detected by EGFP-positive cell bodies in the substantia nigra, and retrograde transport by corticostriatal neurons would be detected by EGFP-positive neurons in regions of neocortex distant from the site of injection. At 14 days post-injection, the rats were killed and the brains were fixed, sectioned and examined for EGFP expression. To reveal whether these viruses were capable of transducing neurons, brain sections were stained immunofluorescently using antibodies against the neuron-specific nuclear protein (NeuN).

Examination of the striatum using fluorescence microscopy revealed that both vesicular stomatitis virus G protein (VSVG) and rabies pseudotyped vectors showed strong tropism for neurons with EGFP clearly visible in striatopallidal axons (Figures 1b and e). The sections were also stained with NeuN (Figures 1c and f). Colocalization of EGFP with NeuN-positive cells confirmed the neuronal tropism of these pseudotyped viruses (Figures 1d and g). Interestingly, vector pseudotyped with gp64 envelope demonstrated a very different tropism in the striatum, preferentially transducing cells of astroglial lineage (Figure 1h) and no colocalization of EGFP was observed with the NeuN-labelled neurons (Figures 1i and j). The staining of sections with antibodies against the astrocyte-specific glial fibrillary acid protein (GFAP) showed that EGFP expression (Figure 1k) colocalized with the labelled astrocytes (Figures 1l and m).

Examination of the substantia nigra revealed that neither VSVG nor gp64 pseudotyped virus had any retrograde transport abilities following their injection into the striatum. Rabies pseudotyped virus resulted in a very small number of EGFP-positive cells in the substantia nigra and regions of neocortex distant from the site of injection, suggesting that some retrograde transport was taking place but with a limited efficiency. No EGFP expression was detected in the contralateral hemisphere using any of the pseudotyped vectors, suggesting that viral spread from the site of injection is limited and does not cross over into the contralateral hemisphere of the brain.

#### *In utero gene delivery and long-term expression using pseudotyped NILV vectors*

Having observed that VSVG and rabies pseudotyped NILVs target neurons and gp64 pseudotype targets astrocytes in adult rodents, we wanted to establish whether this was the case in the immature brain of mice *in utero* before it has fully taken on its post-mitotic character. Each pseudotyped lentivirus, 5  $\mu$ l (of the same stock used in adult rats), was injected, *in utero*, into the brains of fetal MF1 mice at embryonic (E) day E14. Born mice were reared until P21 before being killed and the brains removed, fixed and sectioned. EGFP expression was detected using anti-EGFP antibodies and diaminobenzidine dihydrochloride (DAB) staining.

Light microscopy examination of the tissue sections revealed that VSVG pseudotyped vector transduced pyramidal neurons in the cingulate cortex, as shown by strong EGFP staining (Figure 2b). Lower power magni-

fication showed the wide areas of transduction including the sensorimotor cortex (Figure 2c) and, interestingly, staining was observed in both hemispheres of the brain. These findings are in contrast to what we had observed in the adult rats where viral spread through the parenchyma was much less extensive. Examination of the hippocampus also revealed extensive transduction of pyramidal neurons in CA1-3 and a smaller number of neurons in the dentate gyrus (Figure 2d). High-power magnification of a stained cell shows the typical morphology of a cortical neuron with stained cell body and associated axon and dendrites (Figure 2e). Rabies pseudotyped vector also showed neuron-specific transduction in the cortex (Figures 2g, h and j). However, although transduced neurons were observed in the cortex in both hemispheres, the efficiency of transduction was clearly much less than that seen using VSVG pseudotype. Similarly, low levels of neuron-specific transduction were seen in the hippocampus (Figure 2i). Fetally administered vector pseudotyped with gp64 envelope produced little or no transduction of neural cells in the cortex (Figures 2l and m) or hippocampus (Figure 2n). Interestingly, the few EGFP-positive cells found in the cortex displayed neuronal morphology (Figure 2o), with no visible transduction of astrocytes.

To confirm the neuronal nature of transduced cells sections of brains that were transduced by VSVG pseudotyped NILV *in utero* were stained with 4,6-diamidino-2-phenyl indole (DAPI) to identify nuclei (Figure 3a) and with Neurotrace to identify neurons (Figure 3b). EGFP-positive transduced cells were clearly visible (Figure 3c). EGFP-positive cells colocalized with Neurotrace-stained cells to produce a yellow colour surrounding the cell soma (Figure 3d). Figure 3e shows an orthogonal image of EGFP-positive cells that are colocalized with DAPI and Neurotrace. We also stained adjacent sections with the astrocytic-specific antibodies against GFAP (Figure 3g) together with DAPI (Figure 3f) and EGFP to label transduced cells. Although EGFP-positive cells were clearly visible (Figure 3h), when signals were merged there was no colocalization of EGFP-positive cells with GFAP-stained cells (Figures 3i and j).

We were interested in establishing whether gene expression was maintained over a longer period of time, as it was possible that episomal templates would not be stable and could be diluted out in a developing nervous system. Therefore, mice injected *in utero* with VSVG pseudotyped vector were left for 4 months after birth before being killed and the brain extracted, fixed and sectioned. The brain sections were again stained with DAPI (Figure 3k) and Neurotrace (Figure 3l). Strong expression of EGFP in transduced cells was clearly evident (Figure 3m). Multichannel confocal microscopy confirmed that this EGFP expression was within neurons (Figure 3n). This was also seen in orthogonal images (Figure 3o). Long-term and strong expression of EGFP within pyramidal neurons of the cortex was also observed using this method (data not shown).

#### *Stereological quantification of transduced neurons following in utero delivery of ILV and NILV vectors to the fetal mouse brain*

Confirmation of the ability of VSVG pseudotyped NILV to efficiently transduce neurons following *in utero*

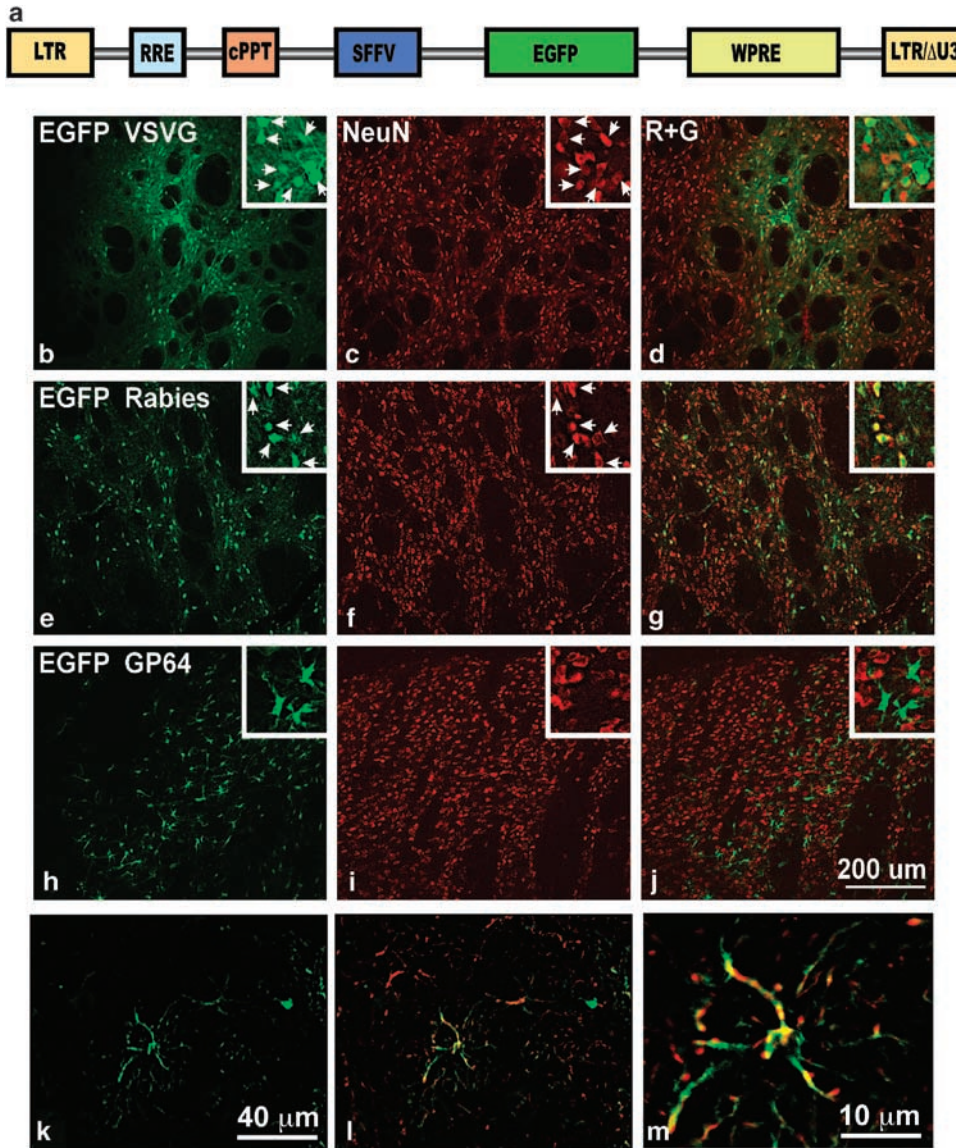


**Figure 1** Cell-specific gene delivery to rat corpus striatum using pseudotyped non-integrating lentivirus (NILV) vectors. (a) Schematic representation of the HIV-1-based vector used in this study (LTR, long terminal repeat; RRE, rev response element; cPPT, central polypurine tract; SFFV, spleen focus-forming virus promoter; EGFP, enhanced green fluorescent protein; WPRE, woodchuck hepatitis virus post-transcriptional regulation element). The NI lentiviral vectors were pseudotyped with vesicular stomatitis virus G protein (VSVG), rabies and gp64 envelopes and stereotactically injected in corpus striatum of adult rats. At 14 days post-injection the brains were sectioned and gene delivery was evaluated by fluorescent microscopy. EGFP expression was seen throughout the striatum with efficient transduction of striatopallidal axons when using VSVG pseudotyped virus (b). Neuronal expression was confirmed by staining neurons with neuron-specific nuclear protein (NeuN) (c). Cells that were visibly EGFP positive and NeuN labelled under higher magnification are highlighted by the white arrows in the insets of each panel. The merging of EGFP-positive cells with NeuN-labelled cells produced a yellow colocalized signal (d). Rabies pseudotyped vector also transduced neurons (e), which was also confirmed by costaining with NeuN (f). The insets in the panels show cells under higher magnification with white arrows to highlight cells that are EGFP positive and NeuN labelled. The merging of colocalized signal produced yellow cells (g). Vectors pseudotyped with gp64 transduced astrocytes and these were identifiable by their distinct morphology (h and k). Costaining of sections with NeuN (i) showed no colocalization of signal with EGFP-positive astrocytes (j). Astrocyte tropism was confirmed by costaining with GFAP antibodies and colocalization with EGFP expression producing yellow signal (l and m).

intracranial administration at E14 led us to investigate how this would compare to an ILV. ILV and NILV were produced and titre matched ( $25 \text{ ng ml}^{-1}$ ) using a reverse transcriptase (RT) assay before being administered *in utero* through intracranial injection, as previously described (NILV injections  $n=5$ , ILV injections  $n=4$ ). The mice were killed at P21 and the brains were

extracted, fixed and sectioned. The sections were immunofluorescently stained for the presence of EGFP. Strong EGFP expression was seen in neurons of the brains injected with both ILV and NILV including the primary motor cortex (M1), as shown in Figures 4a and b, respectively. Using StereoInvestigator software, the number of EGFP-positive neurons in the M1 was

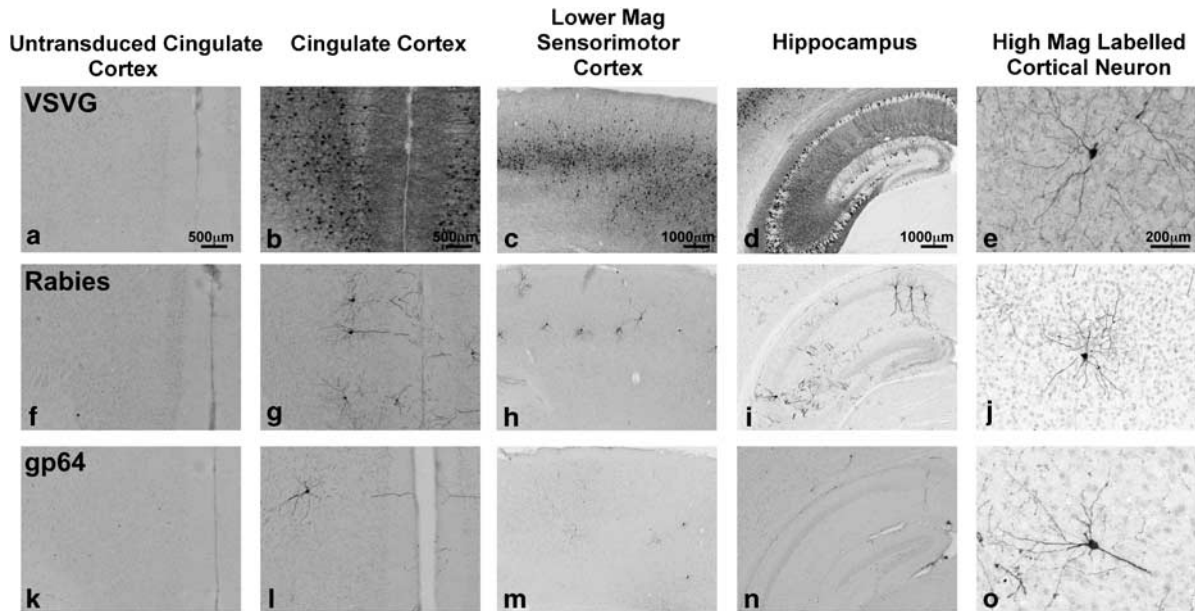


**Figure 2** Gene delivery to the mouse fetal brain following *in utero* administration of pseudotyped non-integrating lentiviruses (NILVs). Pseudotyped NILVs were administered *in utero* through intracranial injection into the brains of E14 fetal mice. The mice were killed at P21 and brain sections were stained using primary antibodies against enhanced green fluorescent protein (EGFP) and diaminobenzidine dihydrochloride (DAB) staining. Microscopic analysis revealed efficient and extensive transduction of pyramidal neurons in the cerebral cingulate (b) and sensorimotor cortex (c) of brains injected with vesicular stomatitis virus G protein (VSVG) pseudotyped NI vector. Examination of the hippocampus also revealed efficient and extensive staining of neurons (d). Higher power magnification showed EGFP had spread from the cell body of individual cortical neurons to the associated dendrites and axon (e). The rabies pseudotyped virus produced a similar pattern of cell tropism to VSVG and transduced neurons in the cortex although the efficiency of transduction was clearly lower (g and h). In the hippocampus, neurons were transduced but again at lower efficiency compared to that seen using VSVG pseudotype (i). Higher power magnification showed that the neurons that were transduced expressed EGFP strongly that spread throughout the cell (j). Brains injected with gp64 pseudotyped virus produced very low levels of transduction and the few cells that were EGFP positive in the cortex were neurons (l and m). Examination of the hippocampus showed little or no transduction of cells (n). The few cells that were transduced showed strong staining of EGFP throughout the cell (o). All figures are representative of successful injections.

quantified. The data collated showed broad variation in cell counts from one mouse to another in each group (Figure 4c). Of the four mouse fetuses injected with ILV, one showed no trace of EGFP-positive cells in the M1 and so would be regarded as a failed injection. Of the five fetuses injected with the NILV, two of these were regarded as failed injections.

Interestingly, although both ILV and NILV were administered by a single injection into the left hemisphere of the fetal brain, strong and widespread EGFP expression could also be seen on the contralateral side. Figures 4d and e show efficient staining of neurons in the cortex in both hemispheres using ILV and NILV, respectively.

#### Quantification of expression and copy number analysis following stereotactic administration of ILV and NILV to the adult mouse brain

Titre matched ILV and NILV were administered by bilateral stereotactic injection to corpus striatum of adult mice ( $n = 5$ ). All mice survived the procedure with the no noticeable adverse effects to the injected viruses. At 1 month post-injection, the mice were killed and the brains were extracted and bisected along the midline. One hemisphere was fixed, sectioned and stained for EGFP expression. Examination of DAB-stained sections revealed strong EGFP expression localized to the site of injection for both NILV and ILV (Figures 5a and b,

respectively;  $\times 10$  magnification). This limited viral spread was similar to that observed in our previous administrations to adult rats (Figure 1) and in stark contrast to that seen following *in utero* administration to fetal mouse brains (Figures 3 and 4). Gene expression from ILV and NILV was measured by quantitative thresholding image analysis of EGFP immunoreactivity using Image Pro-Plus software. The data were plotted as the mean % immunoreactivity per  $0.01 \text{ mm}^2$  (Figure 5c). There was no statistically significant difference between the mean percentage of GFP immunoreactivity between adult mice injected with NILV or ILV.

Genomic DNA was extracted from the other hemisphere of the harvested brains. Viral copy numbers were quantified by qPCR using primers that anneal to the woodchuck post-transcriptional regulatory element (WPPE) sequence. Primers and probes specific for the mouse *titin* gene enabled normalization between samples by calculating the number of cells used in the input. Statistical analysis of the data (Figure 5d) concluded that there was no significant difference between the mean copy number in adult mice injected with NILV and ILV.

#### Transduction of the corticospinal and rubrospinal tract

We investigated the ability of VSVG pseudotyped NILV vector to deliver EGFP to corticospinal neurons. The vector was stereotactically injected into the motor cortex of adult rats ( $n = 5$ ). At 14 days post-injection, the rats were killed and the brain and spinal cord were extracted,

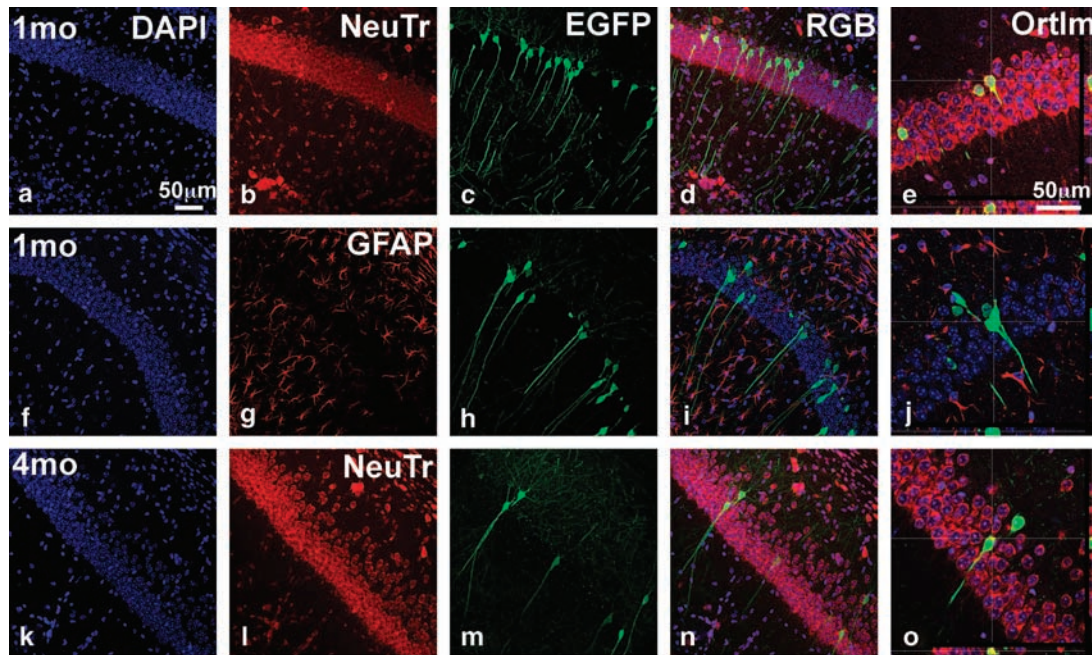


**Figure 3** Immunofluorescent and confocal studies confirming long-term and neuron-specific gene delivery in the hippocampus following *in utero* delivery of non-integrating lentiviruse (NILV). The brain sections of mice that were injected at E14 with vesicular stomatitis virus G protein (VSVG) pseudotyped NILV and killed at P21 were stained with 4,6-diamidino-2-phenyl indole (DAPI) to fluorescently label DNA content of cell nuclei blue (a) and with Neurotrace to label Nissl bodies of neurons red (b). Cells expressing enhanced green fluorescent protein (EGFP) were clearly visible in CA1-3 (c) and merging of images showed colocalization of Neurotrace signal with EGFP-positive cells producing a yellow signal in the cell (d). This was also seen in orthogonal images of cells showing colocalization of signals around the cell soma (e). To further confirm neuronal expression and exclude other cell types, we again stained sections with DAPI (f) but this time labelled astrocytes red using antibodies against glial fibrillary acid protein (GFAP) (g). Strong EGFP expression was detected in cells (h) and merging of signals did not produce colocalization of GFAP-labelled astrocytes with EGFP-positive cells (i). This was also seen in orthogonal images (j). Long-term gene expression was confirmed by staining sections of brains from mice killed 4 month after *in utero* administration of NILV with DAPI (k) and Neurotrace (l). Strong and sustained EGFP expression was seen in cells (m). Merging of signals showed colocalization of Neurotrace signal and EGFP confirming neuron-specific transduction (n) also visible in orthogonal images surrounding the cell soma (o).

fixed and sectioned. Examination of the sections by fluorescence microscopy showed extensive transduction of pyramidal neurons in the cortex, including layer V (Figure 6a). This was confirmed by staining of the slides with NeuN marker (Figure 6b) and colocalization with EGFP (Figure 6c). EGFP expression could be seen in axons leaving the cortex (indicated by the white arrows in Figures 6a and c) and extending into white matter, internal capsule, thalamus, pons, the pyramidal decussation and into the spinal cord as seen in longitudinal sections (Figure 6d) and cross sections (Figure 6e). The strong levels of EGFP signal in the spinal cord suggested that efficient anterograde transport of the protein had occurred along the corticospinal tract originating from the cell bodies of layer V pyramidal neurons in the cortex. To confirm this, we applied a retrograde tracer, FluoroGold (FG) onto the corticospinal tract in the left dorsal funiculus at segmental level cervical vertebrae 3 (C3), 1 week after viral injection into the motor cortex. This was followed by another 7 days survival to allow for retrograde transport of the fluorescent tracer to the contralateral (right) motor cortex and resulted in a sizeable population of EGFP- and FG-positive, double-labelled pyramidal neurons, typically with a moderate level of EGFP expression in their neuronal cell body (Figures 6g-i). Quantification of the EGFP- and FG-positive neurons inside the 0.5 mm region of lentiviral

transduction in the injected motor cortex revealed EGFP expression in  $21 \pm 3\%$  (mean  $\pm$  s.e.m.,  $n = 3$ ) of the FG-positive, retrogradely labelled pyramidal neurons.

To investigate transduction of the rubrospinal tract, VSVG pseudotyped NILV was stereotactically injected into the red nucleus of adult rats and after 14 days the rats were killed and the spine was extracted, fixed and examined by fluorescent microscopy. EGFP expression was seen in axon fibres of the rubrospinal tract passing through the lateral funiculus of the spinal cord at C3 (Figure 6f). Again, the strong EGFP fluorescence in the spinal cord suggested efficient anterograde transport of this protein along the rubrospinal tract. Although there was visible variation in transduction efficiency, in the best animal 519 green axons were counted in one rubrospinal tract. This compares with about 1200 known rubrospinal neurons projecting into each tract.<sup>8</sup>

#### Microglial response to pseudotyped NILVs

The host immune response to a gene therapy vector is of vital importance in evaluating its safety and efficacy. Therefore, we investigated this in terms of immunoreactivity of microglia to VSVG pseudotyped vector. The vector was stereotactically injected unilaterally into the adult rat striatum as described above ( $n = 5$ ). At 14 days post-injection, the brains were extracted, fixed and sectioned and subsequently stained using OX-42,

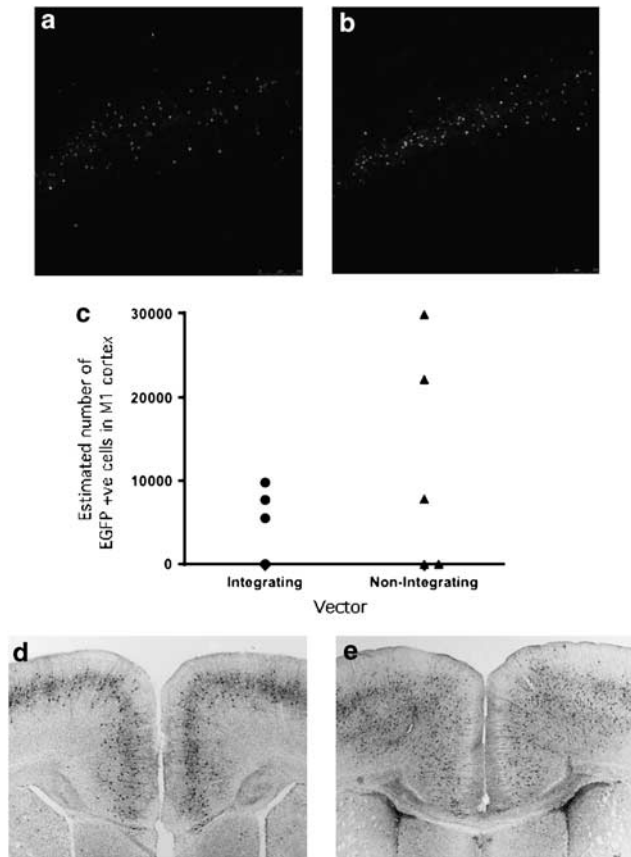


**Figure 4** A comparison between integrating lentivirus (ILV) and non-integrating lentivirus (NILV) transduction following *in utero* administration to the fetal brain. Titre matched ILV and NILV was administered *in utero* to mouse fetal brains through intracranial injection at E14. The brains were harvested at P21 and sectioned before being immunofluorescently stained for the detection of enhanced green fluorescent protein (EGFP)-positive neurons. Strong EGFP expression was observed by confocal microscopy using ILV (a) and NILV (b) in the primary motor cortex (M1). *StereoInvestigator* software was used to quantify transduced neurons in the M1 (c). The Gundersen coefficient of error (CE) for these estimates was  $\leq 0.09$ . A broad variation in data was seen in both groups with one of the four mice injected with ILV representing a failed injection. Two of the five mice injected with NILV were failed injections. Both ILV and NILV vectors transduced neurons in both hemispheres of the brain as shown in (d) and (e), respectively.

anti-integrin  $\alpha M$  (CD11b) antibody, to detect microglial immunoreactivity. The extent of CD11b immunoreactivity was determined by comparison of OX-42 staining in the injected versus uninjected striatum by fluorescence microscopy. As expected, efficient EGFP expression was seen in the striatum (Figure 7a) and OX-42 staining revealed that there was no observable difference in microglial activation areas in which EGFP was either present or absent (Figure 7b). Furthermore, there was also no observable difference between the intensity of OX-42 staining compared to the contralateral uninjected side (Figure 7c). Examination of these OX-42-stained sections under lower magnification revealed microglial activation, in the form of enhanced staining and withdrawal of processes, along the needle tract where some tissue damage would have taken place (as indicated by the white arrow in Figure 7e). Beyond the

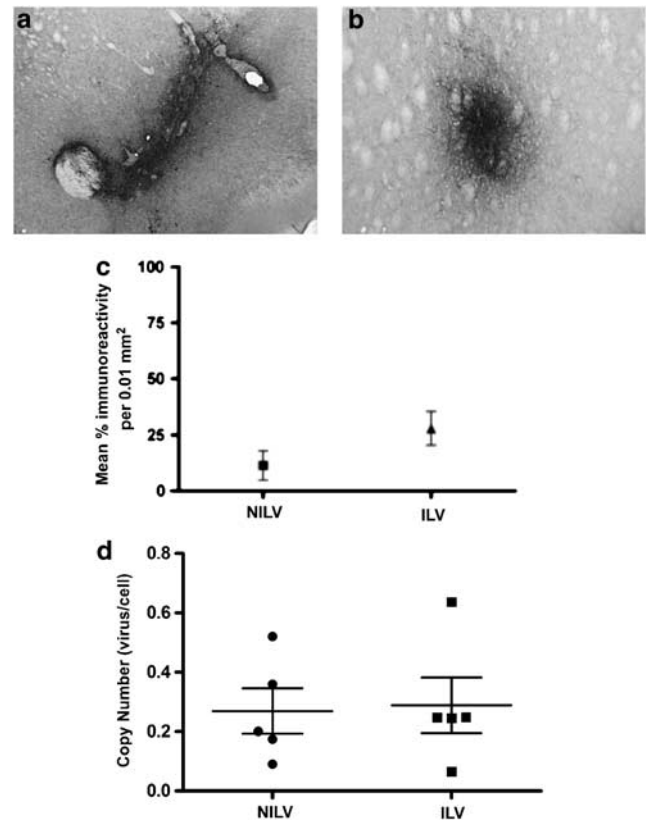


**Figure 5** A comparison between integrating lentivirus (ILV) and non-integrating lentivirus (NILV) transduction following stereotactic administration into adult mouse corpus striatum. Titre matched ILV and NILV was stereotactically injected bilaterally into the corpus striatum of adult mice. The brains were harvested 1 month post-injection and cut along the midline. One hemisphere was diaminobenzidine dihydrochloride (DAB) stained for the detection of enhanced green fluorescent protein (EGFP)-positive cells. Intense staining of EGFP was detected localized around the site of injection for both NILV and ILV (a and b, respectively). Quantitative thresholding image analysis was used to compare EGFP expression from ILV and NILV and plotted as the mean  $\pm$  s.e.m. (c). Statistical analysis using Student's *t*-test showed no significant difference between the means of the two groups of data ( $P=0.05$ ). Viral copy number analysis was carried out by qPCR of DNA extracted from the other hemisphere of the brain and plotted as individual points with the heavy bar indicating the mean and lighter bars indicating  $\pm$  s.e.m. (d). Statistical analysis using Student's *t*-test showed no significant difference between the means of the two groups of data ( $P=0.05$ ).

needle tract, there was no significant microglial response to VSVG and this was more clearly seen when merging the images to appreciate viral spread and lack of enhanced staining in areas distal to the site of injection (Figure 7f).

## Discussion

Lentiviral vectors have been widely used for gene delivery to the CNS for both basic research and experimental therapies targeting a number of neurological disorders.<sup>9,10</sup> The appeal of lentiviral vectors lies in their ease of production, large cloning capacity, low immunogenicity and the fact that they can be readily

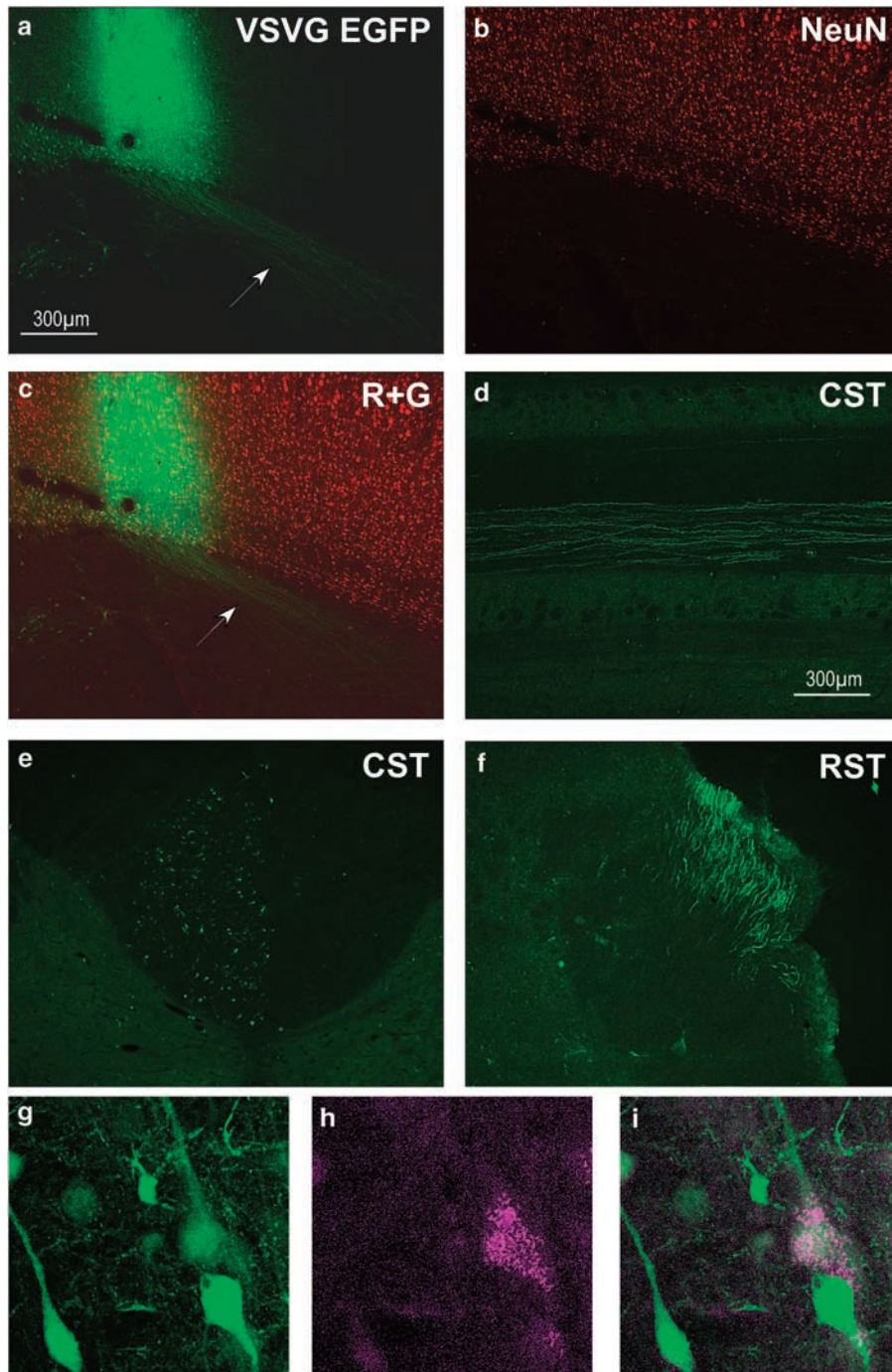


**Figure 6** Gene delivery to the corticospinal and rubrospinal tracts of adult rats. Vesicular stomatitis virus G protein (VSVG) pseudotyped non-integrating lentivirus (NILV) vector was stereotactically injected into the motor cortex of adult rats. At 14 days post-injection the brains and spinal cords were harvested and sectioned. The brain sections were immunofluorescently stained using neuron-specific nuclear protein (NeuN) antibodies to identify neurons and examined by fluorescent microscopy. Pyramidal neurons in the cortex were efficiently transduced including those in layer V (a). Enhanced green fluorescent protein (EGFP) expression in these neurons highlighted the associated corticospinal tract (CST) axons leaving the cortex (white arrow) and extending into the white matter, internal capsule, thalamus, pons, pyramidal tract decussations and into the spinal cord. NeuN antibodies efficiently labelled neurons in the cortex (b) and colocalization with EGFP confirmed neuronal transduction by the virus (c). The EGFP-positive axons of the corticospinal tract were also observed throughout longitudinal sections of the spinal cord (d) as well as in the cross sections at cervical segment 3 (C3) (e). Stereotactic injection of the virus into the red nucleus of adult rat brain resulted in EGFP-positive axon fibres of the rubrospinal tract (RST) in the lateral funiculus, on transversal sections of C3 spinal cord, 14 days after viral injection (f). Application of FluroGold (FG, purple) onto corticospinal tract at C3, 7 days following viral injection into motor cortex also resulted in retrograde labelling of a subpopulation of moderately EGFP-positive pyramidal neurons in the transfected motor cortex (g, EGFP; h, FG; i, double labelling).

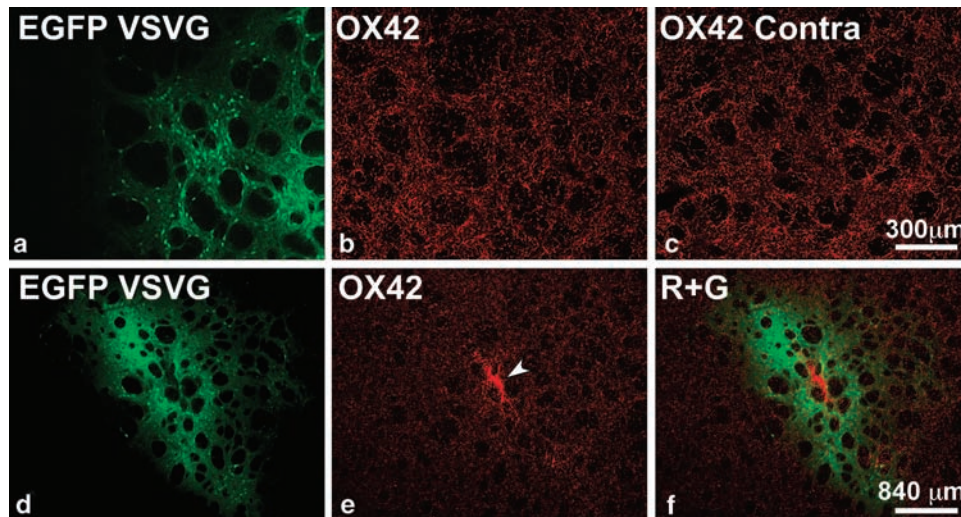


**Figure 7** Microglial-mediated immune response to pseudotyped non-integrating lentivirus (NILV) in rat corpus striatum. Vesicular stomatitis virus G protein (VSVG) pseudotyped NILV was stereotactically injected into rat striatum. At 14 days post-injection the brains were harvested, sectioned and stained using OX-42 antibodies. Fluorescence microscopy revealed strong enhanced green fluorescent protein (EGFP) expression in the striatum (a and d). No observable difference was seen in intensity of staining when comparing areas that are EGFP positive and negative (b). There was also no observable difference in staining intensity when compared to the control contralateral side (c). Lower magnification of the section showed enhanced staining of microglia along the needle tract, as indicated by the arrow (e). Merging of the EGFP and OX-42 signal shows extent of viral spread from site of injection and lack of enhanced OX-42 stain in associated areas (f).

pseudotyped to broaden or limit host transduction range. Indeed, their ability to transduce post-mitotic cells such as neurons and slowly dividing cells such as astrocytes makes them ideal gene delivery vectors for use in the CNS.

The risk of insertional mutagenesis when using lentiviral vectors has been the focus of much research. In a review by Jakobsson and Lundberg,<sup>10</sup> the authors comment on the importance of avoiding insertional mutagenesis if lentiviral vectors are to be used clinically to treat neurological diseases. Although it is not clear what effect insertional mutagenesis would have on post-mitotic neurons, glial cells proliferate and the CNS also contains a limited source of neural stem cells. NILV do not integrate but persist as various transcriptionally functional episomal species, thereby providing an enhanced safety profile with respect to mutagenesis. Yanez-Munoz *et al.*<sup>6</sup> showed that a VSVG pseudotyped NILV transduced neurons in the striatum and hippocampus with sustained gene expression 1 month post-injection. Philippe *et al.*<sup>7</sup> have also shown transduction of neurons in the striatum using a similar NILV. Taken together, these studies have provided an important proof of principle to the possibility of using these viruses in the CNS. Here, we have extended these studies in terms of anatomical site, developmental stage, duration of gene expression and vector pseudotype.

The ability to selectively target neurons is desirable, for example to replace defective ion channels, whereas transduction of glial cells may be desirable if a secreted protein needs to be delivered to a specific location in the brain. Two main methods have been used to achieve cell-specific transduction: cell-specific promoters and virus pseudotyping. Cell-specific expression in the brain using lentivirus has been shown using a number of promoters such as those for enolase<sup>11</sup> and synapsin I<sup>12</sup> for neuronal-

specific expression and human GFAP promoter for glial-specific expression.<sup>11</sup>

In this study we have explored pseudotyping to achieve cell specificity. A broad range of viral envelopes to pseudotype lentiviral vectors has been used to examine cell tropism in the brain. Using an equine infectious anaemia virus-based lentiviral system, Mazarakis *et al.* reported that pseudotyping with VSVG led to preferential neuronal gene delivery. In addition to this, rabies virus pseudotype exhibited retrograde transport properties.<sup>13,14</sup> In terms of an HIV-1-based lentiviral system, the preferential tropism of VSVG pseudotyped virus for neurons has been previously observed in rodents<sup>15,16</sup> and non-human primates.<sup>17</sup> However, when injected specifically into white matter cells of all major macroglial types are transduced.<sup>18</sup> Consistent with these studies, transduction patterns in corpus striatum in adult rats showed that VSVG and rabies pseudotyped NILV preferentially transduce neurons. In contrast, a baculoviral-derived gp64 pseudotype showed no neuronal tropism, and preferential transduced cells of astrocytic lineage.

The widespread gene delivery observed after *in utero* administration is an important finding and may be applicable to treat diseases such as lysosomal storage diseases. At E14, the mouse CNS is still immature and developing and there is a dynamic mix of dividing, newly generated, migrating, differentiating and differentiated neurons present; for example in the mouse cerebral cortex neurogenesis starts at E11 and continues until E17.<sup>19</sup> However, these neurons clearly express the necessary receptors on their cell membranes that are required for cell entry. Fetal gene therapy is an attractive principle in that pre-natal intervention may prevent the pathology of early-onset disease, induce tolerance against an expressed therapeutic protein and increase

the likelihood of transducing stem cell populations. The case for this approach is discussed by Coutelle *et al.*,<sup>20</sup> who highlighted a number of animal disease models in which fetal gene therapy has been successful.

The evaluation of pseudotyped NILV vectors in the brains of fetal mice at E14 therefore provides interesting new information. Although administration of the virus using this technique is not as accurate as stereotactic injection in adults (in terms of precise injection in to discrete areas of the brain), every effort was made to inject into approximately the same area of the forebrain. No adverse side effects to the procedure were observed in the mice that came to term. Examination of the mice brains injected with VSVG pseudotyped vector revealed widespread EGFP expression in neurons of the cortex and hippocampus throughout both hemispheres of the brain. Indeed, strong and sustained EGFP expression in neurons was confirmed in mice 4 months after birth. A similar pattern of neuronal tropism in the cortex and hippocampus was seen when using rabies pseudotyped virus, but the efficiency of transduction was clearly lower compared with VSVG pseudotype. Vector pseudotyped with gp64 exhibited poor transduction efficiency with just a few cells expressing EGFP in the cortex. In marked contrast to our findings in gp64-injected adult brains, these cells were neurons with no transduced astrocytes visible. This can be explained by radial glial cells forming astrocytes later in development as gliogenesis commences at E17 in the mouse cortex.<sup>21</sup>

A comparison between NILV and ILV showed no significant differences in transduction efficiency or cell tropism. The VSVG pseudotyped integrating vector also preferentially transduced neurons when administered *in utero* in both hemispheres of the brain following a single injection. The stereological quantification of transduced neurons in the M1 using both ILV and NILV vectors revealed broad variation in the data. Because the batches of virus were titre matched using an RT assay, it is likely that the variation is due to the injection technique. As mentioned, it is difficult to predict where in the forebrain the virus is being administered to and it is possible that some may be lost to an undesirable area such as a ventricle. Also, unlike during the stereotactic injection, the Hamilton syringe is held manually. A measured slower rate of administration is therefore difficult to maintain and the needle cannot be left in position for a period of time after injection to allow virus to disseminate into the brain parenchyma and prevent it from travelling back up the needle tract. Due to variations in the site of injection when administering virus to the fetal brain, we also compared NILV with ILV in adult mouse brains using the more controlled stereotactic injection into the corpus striatum. The highly localized and intense EGFP expression made stereological quantification difficult so quantitative thresholding image analysis of EGFP immunoreactivity was used to compare gene expression. No significant difference in expression between NILV and ILV was found. Viral copy number analysis by qPCR also revealed no significant difference between the two viruses. This data would suggest that NILV perform comparably to ILV in the mouse CNS over the time period we have looked at. Although EGFP expression 4 months after *in utero* injection seemed qualitatively comparable to what we see at 1 month post-injection, longer-term studies are required with compar-

ison to ILV to fully evaluate the application to larger animal models. Such a study would also have to address other confounding factors such as promoter methylation, that is, is the promoter in an NILV more or less prone to silencing given its episomal status?

Stereotactic injections into both adult rat and mouse brains showed limited spread from the site of injection. Widespread transduction of neurons in both hemispheres of the brain was seen following *in utero* administration. A combination of the relatively large volume of virus that was injected and tolerated plus the reduced connective tissue in the E14 mouse brain may account for this increased viral spread compared to the adult models.

Spinal cord injury (SCI) can result in permanent and severe disability for which there is no established or effective treatment. This is mainly associated with the inability of neurons in the CNS to repair or regenerate their axons post-trauma. The use of viral vectors to express neurotrophic<sup>22</sup> or transcriptional factors<sup>23</sup> in the rubrospinal or corticospinal tracts, respectively, in SCI animal models has produced encouraging results. We have demonstrated efficient gene delivery to both corticospinal and rubrospinal tracts in rats using a VSVG pseudotyped NILV vector administered into the cerebral motor cortex or red nucleus, with approximately 20% transfection rate for the corticospinal, and under optimal conditions, more than 40% for the rubrospinal tract, respectively. These data support the use of NILV vectors in the spinal cord as a potentially safer option for gene delivery to treat SCI.

In this study we have applied differently pseudotyped NILV vectors to various parts of the adult and fetal CNS and demonstrated that efficient long-term expression can be achieved in the absence of microglial activation and inflammation. Utilization of different pseudotypes also offers the opportunity to target different cell populations. We have shown that NILV as well as conventional ILV perform in transducing neurons. These studies encourage the development of NILV as safe vectors for CNS gene therapy.

## Materials and methods

### Plasmids

An HIV-1-based lentiviral system was used in this study. The integrase-deficient second-generation plasmid pCMVdr8.74intD64V, wild-type integrase plasmid pCMVdr8.74 and the viral genome plasmid pHR/SIN-cPPT-SEW have been previously described by Yanez-Munoz *et al.*<sup>6</sup> pHR/SIN-cPPT-SEW contains the EGFP expression cassette driven by the spleen focus-forming virus (SFFV) promoter. The WPRE is also included to enhance viral titres (a schematic representation of this plasmid is shown in Figure 1). The plasmid expressing the VSVG, pVSVG, has been previously described.<sup>24</sup> pLP-RVG expresses the rabies virus glycoprotein, pHCMVwhvGP64 expresses the baculoviral envelope glycoprotein and was kindly provided by Dr Paul McCray Jr, University of Iowa, and is based on the plasmid previously described by Sinn *et al.*<sup>25</sup>

### Cell culture and production of pseudotyped NILVs

Human fetal kidney 293T cells were cultured in Dulbecco's modified Eagle's medium supplemented

with 10% fetal bovine serum and 5% penicillin/streptomycin.

NILVs were produced using a three-plasmid transient transfection system. Plasmid encoding for the viral genome pHR/SIN-cPPT-SEW, the gag-pol packaging plasmid pCMVdR8.74D64V and the required envelope plasmid were used to transiently transfect 293T cells using polyethyleneimine reagent (Sigma-Aldrich, Gillingham, UK). The produced viral particles were concentrated by ultracentrifugation at 23 000 r.p.m. for 2 h in a Sorvall Discovery 100SE using a Surespin 630 rotor. The pellet was re-suspended in OptiMEM 1 (Invitrogen, Paisley, UK) and frozen down at  $-80^{\circ}\text{C}$ .

The HIV RT was quantified by an RT enzyme-linked immunosorbent assay-based assay (Roche) in accordance with the manufacturers' protocol. The quantities obtained using these methods were typically between 6 and  $25\text{ ng }\mu\text{l}^{-1}$ . ILV was produced using the same protocol except the pCMVdR8.74 gag-pol packaging plasmid was used that does not contain the D64V mutation in the integrase gene.

#### *Stereotactic injection of pseudotyped NILVs into adult rat CNS and staining of sections*

All animals were handled according to procedures approved by the UK Home Office and the University College London local ethics committee. Adult Sprague-Dawley rats under isoflurane anaesthesia were placed in a stereotaxic frame. Stereotactic injections were carried out using a  $10\text{ }\mu\text{l}$  Hamilton syringe attached to a micromanipulation pump. All injections were carried out at a rate of  $0.2\text{ }\mu\text{l min}^{-1}$  before the needle was retracted by 1 mm and left for 5 min before complete withdrawal. The following volumes of virus and coordinates of injection (relative to bregma in mm) were used—striatum:  $2\text{ }\mu\text{l}$ , 1 mm anterior, 3 mm lateral, 4 mm ventral; motor cortex: 3 injections of  $1\text{ }\mu\text{l}$ , at 2 mm lateral, 1.5 mm ventral, 0.5, 1.0 and 1.5 mm posterior to the bregma; red nucleus:  $1\text{ }\mu\text{l}$ ,  $-6.0\text{ mm}$  anterior, 0.7 mm lateral,  $-6.5\text{ mm}$  ventral. For FG double labelling, the animals were re-anaesthetized after 7 days, the spinal cord was exposed by laminectomy at C4, the left spinal dorsal column was cut between the dorsal root entry zone and the midline and  $4\text{ mm}^2$  of gelfoam (Johnson and Johnson, Skipton, UK) soaked with  $2\text{ }\mu\text{l}$  of 4% FG (Fluorochrome, Denver, Colorado, USA) applied onto the spinal cord surface.

All animals were killed 14 days after viral injection using sodium pentobarbitone (Sagatal; Rhône Merieux, Harlow, UK). The rats were perfused intracardially using phosphate-buffered saline (PBS), followed by 4% paraformaldehyde and the brains and spinal cords were removed and post-fixed for 2 h in 4% paraformaldehyde at  $4^{\circ}\text{C}$ . The brains were cryoprotected in 30% sucrose overnight, frozen on dry ice and then cut at  $40\text{ }\mu\text{m}$ , for coronal brain and longitudinal and transversal spinal cord sections.

Double labelling of EGFP fluorescent brain sections for neurons was performed using antibodies against NeuN (1:100, 2 h), for astrocytes with polyclonal antibodies against GFAP (Z334 DAKO, 1:500, overnight), and for microglia with using the OX-42 monoclonal antibody against the CD11b/ $\alpha\text{M}$  integrin subunit (Abcam, UK; 1:200, overnight). All incubations with primary antio-

odies were performed in PBS blocking solution bovine serum albumin. The sections were thoroughly rinsed in PBST before applying Alexa 488-conjugated secondary antibodies (1:100; Invitrogen).

#### *In utero intracranial injection of pseudotyped NILVs into fetal mice and staining of sections*

Pregnant female MF1 mice (B&K Universal Ltd, UK) at 14 days gestation were used in this study. Under isoflurane anaesthesia, the uterus was exposed through a full-depth midline laparotomy. A  $5\text{ }\mu\text{l}$  vector was administered by a transuterine injection directed to the anterior horn of the lateral ventricle on the left side of the fetal brain using a 34-gauge needle (Hamilton, Reno, NV, USA) with up to six fetuses were injected per dam. The laparotomy was closed in two stages using interrupted stitches of 6-0 silk suture and the mouse permitted to recover in a warm cage. For end-point analysis, mice were anaesthetized with isoflurane and perfusion-fixed with 4% paraformaldehyde. Brains were then cryoprotected in 30% sucrose in 50 mM Tris-buffered saline (TBS) before cryosectioning at  $40\text{-}\mu\text{m}$ -thick sections using a Leitz 1321 Freezing Microtome (Leica Microsystems, Milton Keynes, UK).

EGFP expression was detected by immunohistochemical staining of the sections. Endogenous peroxidase activity in the sections was blocked by incubation in 1%  $\text{H}_2\text{O}_2$  in TBS solution for 30 min. The sections were then rinsed three times in TBS before blocking of non-specific immunoglobulin binding by incubating sections for 30 min in a solution of 15% normal goat serum (NGS) in TBS-T (TBS solution containing 0.3% Triton X-100). Sections were then incubated overnight at  $4^{\circ}\text{C}$  in rabbit anti-GFP (1:10 000; Abcam, Cambridge, UK) in TBS-T/10% NGS. The following day, the sections were rinsed in TBS and incubated for 2 h in goat anti-rabbit IgG diluted in TBS-T/10% NGS, rinsed again in TBS and incubated for 2 h in a 1:1000 solution of Vectastain avidin-biotin solution (ABC; Vector Labs, UK) in TBS prepared 30 min before use. Subsequently, sections were rinsed again and incubated in a freshly made and filtered 0.05% solution of DAB containing 0.01%  $\text{H}_2\text{O}_2$  to visualize GFP immunoreactivity. The staining reaction was stopped by rinsing in ice-cold TBS. Stained sections were subsequently mounted onto chrome gelatine coated Superfrost-plus slides (VWR, Poole, UK) and left to dry overnight. Sections were then dehydrated in a series of rising concentrations of industrial methylated spirits, cleared in xylene for 20 min and coverslipped using DPX mounting medium (VWR). Sections were subsequently viewed under an Axioskop 2 Mot microscope (Carl Zeiss Ltd) to compare the staining detail and the background of each antisera concentration combination. Representative images were then captured using an AxiocamHR camera, and Axiovision 4.2 software (Carl Zeiss Ltd).

For neuronal labelling, sections were blocked in 15% NGS in TBS-T and then incubated overnight in rabbit anti-GFP. The following day, sections were rinsed in TBS and incubated for 2 h with goat anti-rabbit Alexa 488 (1:1000; Invitrogen). After rinsing, sections were incubated for 20 min in Neurotrace 530/615 in TBS (1:100; Invitrogen), followed by a thorough rinse in TBS overnight. Finally, sections were counterstained with DAPI (1:2000; Sigma-Aldrich, Poole, UK), mounted onto

chrome gelatine coated microscope slides and coverslipped in Vectashield mounting medium (Vector Labs).

A modified protocol was used for astrocytic labelling. Sections were incubated overnight with rabbit anti-GFP and mouse-anti-GFAP in 10% NGS/TBS-T (1:500; Chemicon, UK). After rinsing in TBS, sections were incubated for 2 h with goat anti-rabbit Alexa 488 and goat anti-mouse Alexa 568 (1:1000; Invitrogen). The sections were subsequently rinsed, counterstained with DAPI, mounted onto slides and coverslipped in Vectashield mounting medium. Slides were visualized with a laser scanning confocal microscope (Leica SP5, Leica Microsystems, UK). Confocal z-stacks were captured in the cortex and hippocampus to determine the phenotypic identity of transduced cells.

#### *Stereological quantification of EGFP-positive transduced neurons*

Following immunofluorescent staining of sections for the detection of EGFP-positive cells (as described above), StereoInvestigator software (MBF Bioscience) was used to obtain unbiased optical fractionator estimates of the number of GFP-positive transfected cells in the M1. These estimates were performed as described previously.<sup>26–28</sup> In brief, a random starting section was chosen, followed by every sixth GFP-stained section thereafter. GFP-expressing cells were sampled using a series of counting frames distributed according to a grid superimposed onto the section. The boundaries of the M1 region were defined in reference to landmarks. Only GFP-expressing cells with a clearly visible cell body that fell within the dissector frame were sampled, using a  $\times 40$  objective (NA 1.30). The following sampling scheme was used for the M1 region (grid area 40 000  $\mu\text{m}^2$ ; frame area 14 200  $\mu\text{m}^2$ ). These estimates were obtained blind to the viral vector injected. The Gundersen coefficient of error (CE) for these estimates was  $\leq 0.09$ .

#### *Stereotactic injection of NILV and ILV into adult mouse CNS*

All procedures were carried out under license from the Home Office with the approval of the King's College London Ethical Review Panel and subject to the Animals (Scientific Procedures) Act 1986. Adult MF-1 mice were anaesthetized with isoflurane (4% induction, 2% maintenance) and mounted in a stereotactic frame. Using bregma as reference, bilateral burr holes were made at the following coordinates above the striatum (anterior/posterior +0.5 mm, medial/lateral  $\pm 2$  mm). A 2  $\mu\text{l}$  Hamilton syringe attached to a microinjection pump (UMP III, World Precision Instruments) was descended to a depth of 3 mm from the surface of the brain. A total of 0.25  $\mu\text{l}$  of NILV or ILV was injected at a rate of 0.1  $\mu\text{l min}^{-1}$  into each injection site, and the syringe was left in place for another 3 min to allow diffusion away from the tip.

All animals were left for 1 month before being killed with sodium pentobarbital. The mice were perfused intracardially with chilled PBS, and the brain was removed from the skull and bisected along the midline. One hemisphere was stored in PBS for subsequent qPCR analysis and the other hemisphere was post-fixed for 24 h in 4% paraformaldehyde, cryoprotected in 30% sucrose in 50 mM TBS before cryosectioning at 40- $\mu\text{m}$

thick sections using a Leitz 1321 Freezing Microtome (Leica Microsystems).

#### *Quantitative analysis of lentiviral expression in adult mice*

The expression of NILV and ILV in adult mice was measured by quantitative thresholding image analysis of GFP immunoreactivity as previously described.<sup>26,29</sup> Briefly, 40 non-overlapping images were captured on 4 consecutive sections spanning the injection site of NILV/ILV within the forebrain. Images were captured with a live video camera (JVC, 3CCD, KY-F55B), mounted onto a Zeiss Axioplan microscope using a  $\times 40$  objective. During the capture phase, all parameters including lamp intensity, video camera setup and calibration were kept constant. Captured images were analysed using Image Pro-Plus software (Media Cybernetics) using a semi-automated thresholding method based on the optical density of the immunoreactive product. Foreground immunostaining was accurately defined by averaging the highest and lowest immunoreactivities within the sample population for a selected immunohistochemical marker (per colour/filter channel selected) and measured on a scale from 0 (100% transmitted light) to 255 (0% transmitted light). This threshold was utilized as a constant for all subsequent images to determine the immunoreactive profile for each animal. Macros were recorded to transfer the data to a spreadsheet for statistical analysis. Data were plotted graphically as the mean percentage area of immunoreactivity per field  $\pm$  s.e.m.

#### *Quantitative PCR analysis of viral copy numbers*

Genomic DNA was isolated from brain tissue using the DNeasy kit (Qiagen) following the manufacturer's protocol. The relative amount of proviral DNA in samples was calculated by real-time PCR using an ABI PRISM 7000 sequence detector. Two sets of primers (Invitrogen), TaqMan probes (Eurofins MWG Operon, Ebersberg, Germany) and the relevant standards were designed to determine copy number and were a kind gift from Dr A Galy (Genethon, France).<sup>30</sup> The following were used for amplification of virus-specific WPRE sequence: WPREmut6 forward primer, 5' TGGATTCTGCGCGGGA 3'; WPREmut6 reverse primer, 5' GAAGGAAGGTCGCTGGATT 3'; WPREmut6 probe, (FAM) 5' CTTCTGCTACGTCCCTTCGGCCCT 3' (TAMRA). The second set was specific for the mouse *titin* gene to enable normalization between the samples by calculating the number of cells used as the input: Titin Mex5 forward, 5' aaaacgagcagtgacgtgacg 3'; Titin mex 5 reverse, 5' ttcagtcagctgctagcgc 3'; Titin Probe, (FAM) 5' tgcacggaagcgtctctcagtc 3' (TAMRA).

PCR reactions were performed in 25  $\mu\text{l}$  volumes containing 5  $\mu\text{l}$  of template DNA, 12.5  $\mu\text{l}$  of Platinum-Quantitative PCR Supermix-UDG with Rox (Invitrogen), 0.9 mM primers and 0.2 mM probe. Following the initial steps at 50 °C (2 min) and then at 95 °C (10 min), PCR was carried out for 40 cycles of 95 °C (15 s) and then 60 °C (1 min). Serial dilutions of plasmids containing appropriate sequences to produce a standard amplification curve for quantification were carried out and all samples were tested in triplicate.

## Acknowledgements

We thank Ruth Seabright, University of Birmingham, for providing the pLP-RVG construct and Paul McCray Jr, University of Iowa, for providing the pHCMVwhvGP64 construct. This work was funded by the Biotechnology and Biological Sciences Research Council. SNW (Philip Gray Memorial Fellow) and SMKB are supported by the Katherine Dormandy Trust and NJW is funded by the Medical Research Council. AJT is supported by The Wellcome Trust.

## References

- Hacein-Bey-Abina S, Von Kalle C, Schmidt M, McCormack MP, Wulffraat N, Leboulch P et al. LMO2-associated clonal T cell proliferation in two patients after gene therapy for SCID-X1. *Science* 2003; **302**: 415–419.
- Hacein-Bey-Abina S, von Kalle C, Schmidt M, Le Deist F, Wulffraat N, McIntyre E et al. A serious adverse event after successful gene therapy for X-linked severe combined immunodeficiency. *N Engl J Med* 2003; **348**: 255–256.
- Seggewiss R, Pittaluga S, Adler RL, Guenaga FJ, Ferguson C, Pilz IH et al. Acute myeloid leukemia is associated with retroviral gene transfer to hematopoietic progenitor cells in a rhesus macaque. *Blood* 2006; **107**: 3865–3867.
- Bokhoven M, Stephen SL, Knight S, Gevers EF, Robinson IC, Takeuchi Y et al. Insertional gene activation by lentiviral and gammaretroviral vectors. *J Virol* 2008; **83**: 283–294.
- Philpott NJ, Thrasher AJ. Use of nonintegrating lentiviral vectors for gene therapy. *Hum Gene Ther* 2007; **18**: 483–489.
- Yanez-Munoz RJ, Balaggan KS, MacNeil A, Howe SJ, Schmidt M, Smith AJ et al. Effective gene therapy with nonintegrating lentiviral vectors. *Nat Med* 2006; **12**: 348–353.
- Philippe S, Sarkis C, Barkats M, Mammeri H, Ladroue C, Petit C et al. Lentiviral vectors with a defective integrase allow efficient and sustained transgene expression *in vitro* and *in vivo*. *Proc Natl Acad Sci USA* 2006; **103**: 17684–17689.
- Liu Y, Himes BT, Murray M, Tessler A, Fischer I. Grafts of BDNF-producing fibroblasts rescue axotomized rubrospinal neurons and prevent their atrophy. *Exp Neurol* 2002; **178**: 150–164.
- Wong LF, Goodhead L, Prat C, Mitrophanous KA, Kingsman SM, Mazarakis ND. Lentivirus-mediated gene transfer to the central nervous system: therapeutic and research applications. *Hum Gene Ther* 2006; **17**: 1–9.
- Jakobsson J, Lundberg C. Lentiviral vectors for use in the central nervous system. *Mol Ther* 2006; **13**: 484–493.
- Jakobsson J, Ericson C, Jansson M, Bjork E, Lundberg C. Targeted transgene expression in rat brain using lentiviral vectors. *J Neurosci Res* 2003; **73**: 876–885.
- Hioki H, Kameda H, Nakamura H, Okunomiya T, Ohira K, Nakamura K et al. Efficient gene transduction of neurons by lentivirus with enhanced neuron-specific promoters. *Gene Ther* 2007; **14**: 872–882.
- Wong LF, Azzouz M, Walmsley LE, Askham Z, Wilkes FJ, Mitrophanous KA et al. Transduction patterns of pseudotyped lentiviral vectors in the nervous system. *Mol Ther* 2004; **9**: 101–111.
- Mazarakis ND, Azzouz M, Rohll JB, Ellard FM, Wilkes FJ, Olsen AL et al. Rabies virus glycoprotein pseudotyping of lentiviral vectors enables retrograde axonal transport and access to the nervous system after peripheral delivery. *Hum Mol Genet* 2001; **10**: 2109–2121.
- Naldini L, Blomer U, Gage FH, Trono D, Verma IM. Efficient transfer, integration, and sustained long-term expression of the transgene in adult rat brains injected with a lentiviral vector. *Proc Natl Acad Sci USA* 1996; **93**: 11382–11388.
- Blomer U, Naldini L, Kafri T, Trono D, Verma IM, Gage FH. Highly efficient and sustained gene transfer in adult neurons with a lentivirus vector. *J Virol* 1997; **71**: 6641–6649.
- Kordower JH, Bloch J, Ma SY, Chu Y, Palfi S, Roitberg BZ et al. Lentiviral gene transfer to the nonhuman primate brain. *Exp Neurol* 1999; **160**: 1–16.
- Zhao C, Strappe PM, Lever AM, Franklin RJ. Lentiviral vectors for gene delivery to normal and demyelinated white matter. *Glia* 2003; **42**: 59–67.
- Zhang W, Yi MJ, Chen X, Cole F, Krauss RS, Kang JS. Cortical thinning and hydrocephalus in mice lacking the immunoglobulin superfamily member CDO. *Mol Cell Biol* 2006; **26**: 3764–3772.
- Coutelle C, Themis M, Waddington SN, Buckley SM, Gregory LG, Nivsarkar MS et al. Gene therapy progress and prospects: fetal gene therapy—first proofs of concept—some adverse effects. *Gene Ther* 2005; **12**: 1601–1607.
- Fitzgerald DP, Bradford D, Cooper HM. Neogenin is expressed on neurogenic and gliogenic progenitors in the embryonic and adult central nervous system. *Gene Expr Patterns* 2007; **7**: 784–792.
- Kwon BK, Liu J, Lam C, Plunet W, Oschpik LW, Hauswirth W et al. Brain-derived neurotrophic factor gene transfer with adeno-associated viral and lentiviral vectors prevents rubrospinal neuronal atrophy and stimulates regeneration-associated gene expression after acute cervical spinal cord injury. *Spine* 2007; **32**: 1164–1173.
- Yip PK, Wong LF, Pattinson D, Battaglia A, Grist J, Bradbury EJ et al. Lentiviral vector expressing retinoic acid receptor beta2 promotes recovery of function after corticospinal tract injury in the adult rat spinal cord. *Hum Mol Genet* 2006; **15**: 3107–3118.
- Johnson LG, Mewshaw JP, Ni H, Friedmann T, Boucher RC, Olsen JC. Effect of host modification and age on airway epithelial gene transfer mediated by a murine leukemia virus-derived vector. *J Virol* 1998; **72**: 8861–8872.
- Sinn PL, Hickey MA, Staber PD, Dylla DE, Jeffers SA, Davidson BL et al. Lentivirus vectors pseudotyped with filoviral envelope glycoproteins transduce airway epithelia from the apical surface independently of folate receptor alpha. *J Virol* 2003; **77**: 5902–5910.
- Bible E, Gupta P, Hofmann SL, Cooper JD. Regional and cellular neuropathology in the palmitoyl protein thioesterase-1 null mutant mouse model of infantile neuronal ceroid lipofuscinosis. *Neurobiol Dis* 2004; **16**: 346–359.
- Kielar C, Maddox L, Bible E, Pontikis CC, Macauley SL, Griffey MA et al. Successive neuron loss in the thalamus and cortex in a mouse model of infantile neuronal ceroid lipofuscinosis. *Neurobiol Dis* 2007; **25**: 150–162.
- Pontikis CC, Cotman SL, MacDonald ME, Cooper JD. Thalamocortical neuron loss and localized astrocytosis in the *Cln3<sup>Deltaex7/8</sup>* knock-in mouse model of Batten disease. *Neurobiol Dis* 2005; **20**: 823–836.
- Pontikis CC, Cella CV, Parihar N, Lim MJ, Chakrabarti S, Mitchison HM et al. Late onset neurodegeneration in the *Cln3<sup>-/-</sup>* mouse model of juvenile neuronal ceroid lipofuscinosis is preceded by low level glial activation. *Brain Res* 2004; **1023**: 231–242.
- Charrier S, Stockholm D, Seye K, Opolon P, Taveau M, Gross DA et al. A lentiviral vector encoding the human Wiskott-Aldrich syndrome protein corrects immune and cytoskeletal defects in WASP knockout mice. *Gene Ther* 2005; **12**: 597–606.